

## Total nuclear inelastic electron scattering cross sections compared to sum rule calculations

J. S. O'Connell, E. Hayward, J. W. Lightbody, Jr., and X. K. Maruyama  
National Bureau of Standards, Washington, D.C. 20234

P. Bosted  
American University, Washington, D.C. 20016

K. I. Blomqvist  
Massachusetts Institute of Technology, Cambridge, Massachusetts 02139

G. Franklin  
Carnegie-Mellon University, Pittsburgh, Pennsylvania 15213

J-O. Adler, K. Hansen, and B. Schroder  
University of Lund, Lund, Sweden S-223 62

(Received 19 January 1983)

The nuclear response to 200–350 MeV electrons inelastically scattered at 20° for six nuclei ranging from  $A=9$  to 181 is given. An excitation energy integral is formed and compared with three theoretical calculations of the total inelastic scattering cross section.

[ NUCLEAR STRUCTURE  $Z(e, e')$  with  $Z=4, 6, 13, 23, 40,$  and  $73,$   
measured  $d^2\sigma/d\Omega dE$  at  $\theta=20^\circ$  vs  $E,$  determined  $S_{\text{inel}},$  compared with  
model predictions. ]

### I. INTRODUCTION

The cross section for electron scattering on nuclei is written in the plane wave Born approximation in terms of Coulomb and transverse form factors,  $F_C(q, \omega)$  and  $F_T(q, \omega)$ , which are functions of the momentum,  $q$ , and energy,  $\omega$ , transferred to the nucleus by the electron

$$\frac{d^2\sigma}{d\Omega d\omega} = \sigma_0 \left\{ \frac{q_\mu^4}{q^4} F_C^2(q, \omega) + \left[ \frac{q_\mu^2}{2q^2} + \tan^2 \frac{\theta}{2} \right] F_T^2(q, \omega) \right\}. \quad (1)$$

The quantity  $\sigma_0$  is defined to include the single-particle Mott cross section and the kinematic recoil factor for a target of mass  $M_T$ ,

$$\sigma_0 = \left[ \frac{\alpha \cos \theta / 2}{2E_i \sin^2 \theta / 2} \right]^2 / \left[ 1 + \frac{2E_i \sin^2 \theta / 2}{M_T} \right]. \quad (2)$$

The initial and final electron energies are  $E_i$  and  $E_f$ , the scattering angle is  $\theta$ , and

$$q_\mu^2 = q^2 - \omega^2 = 4E_i E_f \sin^2 \theta / 2.$$

Constants  $\alpha = \frac{1}{137}$  and  $\hbar = c = 1$  are used.

The focus of many  $(e, e')$  studies is the comparison of  $F_C^2$  and  $F_T^2$  measurements for discrete states of definite spin, parity, and isospin with shell model calculations. A more global comparison of measurement and models can be made using the electron scattering cross section integrated over all kinematically available nuclear excitation energies. This kind of comparison is expressed in the language of sum rules. The conclusions of these studies bear on the average properties of nuclei, the fundamental electron-nucleon interaction, and nucleon properties in the nuclear medium.

Recent measurements<sup>1-3</sup> of  $F_C$  and  $F_T$  on a variety of nuclei in the momentum transfer range  $q = 1-2 \text{ fm}^{-1}$  give the appearance that standard models of quasifree electron scattering and the measured nuclear response do not agree. The discrepancy is found in the overestimate by theory of the energy integral of the Coulomb form factor at constant momentum transfer. This quantity, called the Coulomb sum, is given by theory through closure as the expectation value of the square of the Coulomb

operator evaluated in the nuclear ground state. The discrepancies found in Refs. 1 and 2 are being reexamined.

The present experiment was designed to measure the longitudinal nuclear response function in the momentum transfer range around  $q=0.5 \text{ fm}^{-1}$ , where the main nuclear absorption mechanism is excitation of giant multipole resonances. The electron scattering kinematics were chosen to emphasize the charge and longitudinal current mechanisms for exciting the nucleus and to suppress the transverse current and magnetic excitation mechanisms.

## II. CROSS SECTION MEASUREMENTS

The elastic and inelastic electron scattering cross sections of natural targets of Be, C, Al, V, Zr, and Ta were measured at a scattering angle of  $20^\circ$  for incident electron energies of  $E_i=200, 250, 300,$  and  $350 \text{ MeV}$ . The data were taken at the Bates Electron Accelerator Laboratory using the energy-loss spectrometer<sup>4</sup> with multiwire drift chambers backed by a silica aerogel Čerenkov counter<sup>5</sup> to detect the scattered electrons. A transverse wire chamber array provided some measure of angular discrimination against background events associated with instrumental effects such as electrons scattered from the walls of the scattering chamber or from the spectrometer vacuum chamber. Spectrometer magnetic field settings were selected so that each bite of the scattered electron spectrum overlapped the adjacent one by 30%. Thin targets ( $4\text{--}10 \text{ mg/cm}^2$ ) were used to minimize thick target corrections to the data, and ferrite toroids were used to measure the incident electron current.

Elastic scattering cross sections deduced from our data agree reasonably well ( $\pm 2\%$ ) with distorted predictions based on charge distributions derived from previous measurements. Our measured elastic scattering cross sections were used as input to a calculation of the elastic radiation tails discussed in the next section. The inelastic cross sections for the  $350 \text{ MeV}$  incident beam are shown in Fig. 1. Spectra after subtraction of the elastic peak radiative tail are presented in Fig. 2. Peaks due to discrete excited states are not well resolved in these plots because the data are binned in  $100\text{--}200 \text{ keV}$  intervals.

## III. RADIATION TAIL SUBTRACTION

The largest theoretical input required to extract the  $(e, e')$  cross section due to nuclear excitation is the calculation of the radiation tail (RT) associated with the elastic scattering peak. The standard procedure for computing  $d\sigma_{\text{RT}}^2$  is to use the measured elastic cross section times a bremsstrahlung radia-

tion function<sup>6</sup> calculated with electron plane waves, but integrated over the angle of the unobserved photon. A multiple soft photon correction<sup>7</sup> modifies the spectrum near the elastic peak. In our analysis we normalize the computed elastic radiation tail to the data in an energy region that extends between approximately  $1 \text{ MeV}$  away from the elastic peak to the nucleon separation threshold. Discrete inelastic peaks are excluded from the normalization. The normalization leads to agreement between the radiation tail and the data above  $100 \text{ MeV}$ . The normalization for each target element at each incident energy was considered satisfactory if the calculated tail fit the data simultaneously at low and high  $\omega$ . The largest contribution to the uncertainty reflected in our measurement of the sum shown in Figs. 3 and 4 is attributed to the imprecision of determining these normalization factors. At this time we cannot account for the necessity to renormalize the theoretical radiation tail. Theory is generally below experiment for the lighter targets, becoming greater than experiment for the heavy nuclei studied. The normalization factors which are used to multiply the theoretical radiation tails are given in Table I and range from 1.16 for light nuclei to 0.83 for heavy nuclei. Although we expect distortion effects to be important for high- $Z$  nuclei, we cannot rule out the possibility that the normalization is an experimental problem arising, for example, from instrumental scattering which has not been exactly taken into account,<sup>8</sup> dead time effects which affect the elastic peak but are negligible for the inelastic region, target thickness nonuniformity, and the imprecision with which small solid angles are determined. This analysis, however, represents the first attempt to fit radiation tails to electron scattering data over such a large range of  $Z$  and electron energy loss.

Radiation tails due to inelastic scattering modify the shape of the inelastic response function. Radiative corrections to the data shift some strength from high  $\omega$  to low  $\omega$ ; however, the net area under the inelastic spectrum is not sensitive to this correction. Corrections to the carbon  $350 \text{ MeV}$  spectrum show the total area changes by less than 5%. Since other systematic uncertainties are larger than 5% we have not made radiative correction to the inelastic spectra shown in Fig. 2. For the purpose of discussion, in what follows we neglect the small nuclear recoil energy and equate nuclear excitation to electron energy loss.

## IV. INELASTIC SUMS

For each spectrum the elastic radiation tail (shown as the solid line in Fig. 2) was subtracted from the measured cross section. The difference

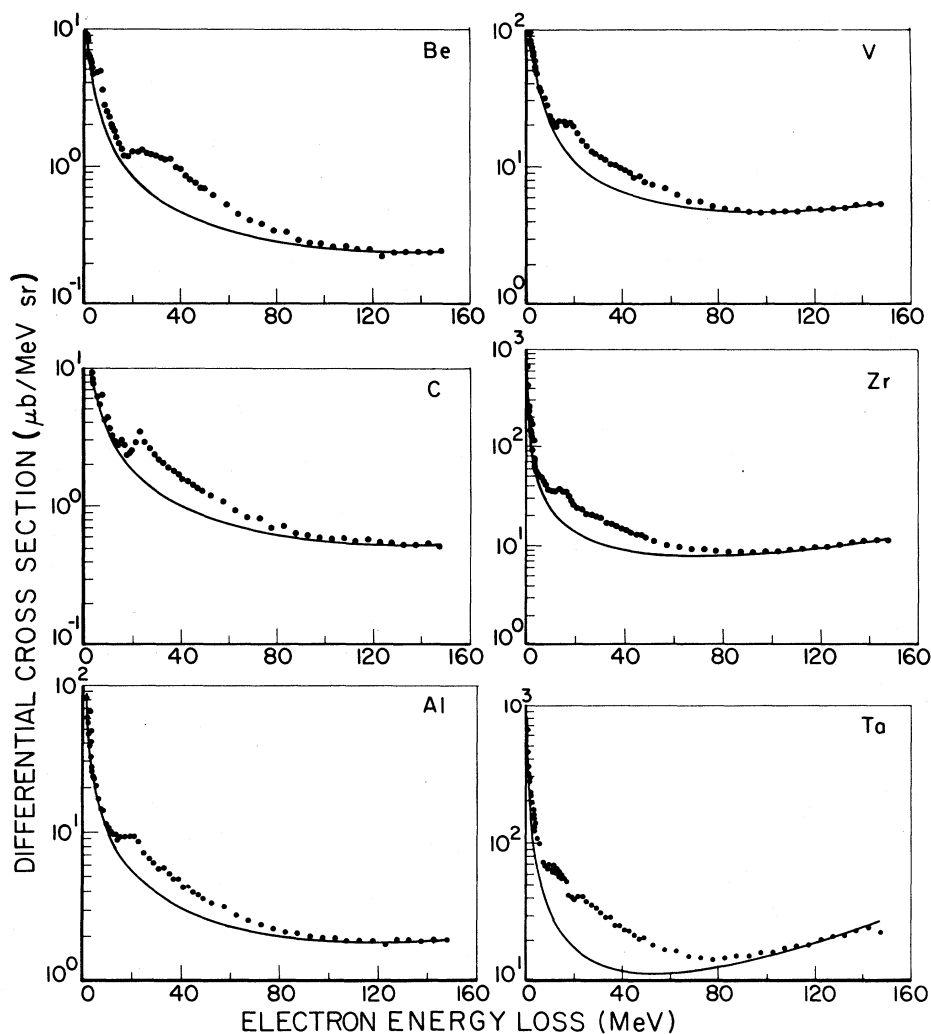


FIG. 1. Inelastic cross sections at  $20^\circ$  for 350 MeV incident electrons. The solid curves are calculated radiation tails from the elastic scattering peaks of each element.

was then divided by the Mott cross section and the kinematical recoil factor to produce the inelastic response

$$F^2(q, \omega) = \left[ \frac{d\sigma_{\text{meas}}^2}{d\Omega d\omega} - \frac{d\sigma_{\text{RT}}^2}{d\Omega d\omega} \right] / \sigma_0. \quad (3)$$

The momentum transfer,  $q$ , is relatively constant across the nuclear excitation region where  $F^2$  is large. The four-momentum transfer,  $q_\mu^2 = q^2 - \omega^2$ , is evaluated at an average excitation energy squared,  $\langle \omega^2 \rangle$ , determined from the measured spectra. The experimental inelastic sum, defined as

$$\begin{aligned} S_{\text{tot}}(q) &= Z^2 F_{\text{el}}^2(q) + Z S_{\text{inel}}(q) \\ &= f_{N^2}(q_\mu^2) \left\{ \left[ \frac{q_\mu^2}{q^4} \right] \mathcal{F}_C^2(q) + \left[ \frac{q_\mu^2}{2q^2} + \tan^2 \frac{\theta}{2} \right] (\mathcal{F}_{T,p}^2(q) + \mathcal{F}_{T,\mu}^2(q)) \right\}, \end{aligned} \quad (5)$$

$$Z S_{\text{inel}}(q) = \int_\epsilon^q F^2(q, \omega) d\omega, \quad (4)$$

can be compared to theoretically evaluated closure sum rules. The lower limit on the energy integral ( $\epsilon$ ) is chosen to exclude the elastic peak; the upper limit is set by kinematics.

## V. THEORETICAL PREDICTIONS

A total electron scattering sum rule (elastic plus inelastic) based on closure over final nuclear states and the plane wave approximation for incident and final electron states can be written as<sup>9-12</sup>

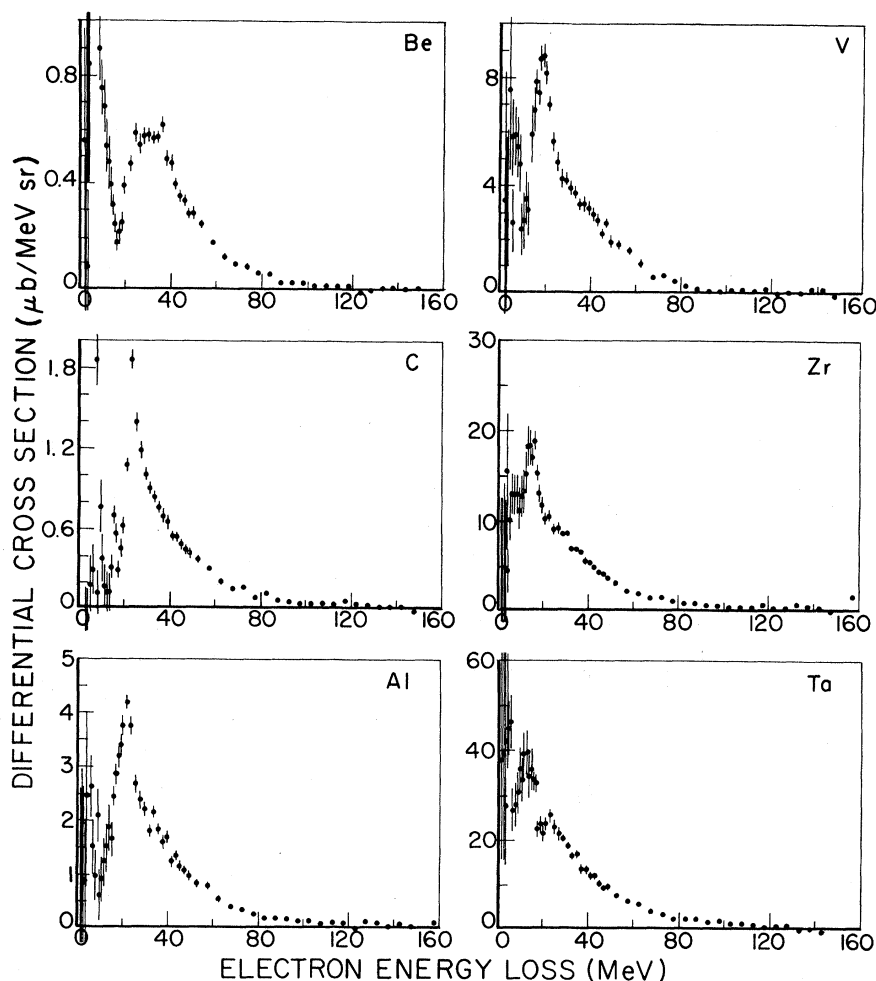


FIG. 2. Inelastic cross sections shown in Fig. 1 after subtracting the elastic radiation tail.

where  $f_N$  is the nucleon form factor and the  $\mathcal{F}$ 's are the form factors, integrated over excitation energy, of the Coulomb, transverse convection current, and spin magnetic moment single-particle operators, respectively,  $(e)\exp(i\vec{q}\cdot\vec{r})$ ,  $(ep_1/M)\exp(i\vec{q}\cdot\vec{r})$ , and  $(\mu\vec{\sigma}\times\vec{q}/2M)\exp(i\vec{q}\cdot\vec{r})$ . Here  $M$  denotes the nucleon mass and  $e=1$  (for a proton) and 0 (for a neutron), and  $\mu$  the nucleon magnetic moment.

To order  $q^2/M^2$  the  $\mathcal{F}$ 's include the Darwin-Foldy term, but not the spin-orbit term<sup>10</sup>; they are expressible in terms of correlation factors,  $f_2$ ,

$$\mathcal{F}_C^2(q) = Z \left[ 1 - \frac{q^2}{4M^2}(2\mu_p - 1) \right] + Z(Z-1)f_2^C(q) \left[ 1 - \frac{q^2}{4M^2} \left( 2\mu_p + \frac{2N}{Z-1}\mu_n - 1 \right) \right], \quad (6)$$

$$\mathcal{F}_{T,p}^2(q) = \frac{2}{3} \frac{Z\langle p^2 \rangle}{M^2} + \frac{2Z(Z-1)}{M^2} f_2^p(q), \quad (7)$$

$$\mathcal{F}_{T,\mu}^2(q) = \frac{q^2}{2M^2} [Z\mu_p^2 + N\mu_n^2 + A(A-1)f_2^\mu(q)]. \quad (8)$$

For the scattering angle and range of momentum transfer covered in the present measurement, the Darwin-Foldy term is not a large contribution, but

in the quasifree region ( $q \geq 1 \text{ fm}^{-1}$ ) it becomes sizable. The  $f_2$ 's are the nucleon pair correlation form factors defined as

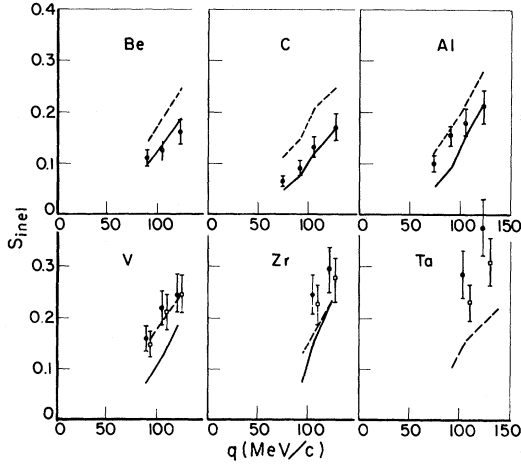


FIG. 3. Inelastic sums as a function of average three-momentum transfer compared with predictions based on the harmonic oscillator (HO) (dashed line) for Be, C, and Al; Fermi gas (FG) (dashed line) for V, Zr, and Ta; and Eq. (17) using photon sum rule data ( $\gamma_{\text{sum}}$ ) (solid line). The data points indicated by the solid circles are the measured  $S_{\text{inel}}$ , whereas those indicated by the open squares are the same data corrected for the effects of Coulomb distortion.

$$Z(Z-1)f_2^C(q) = \sum_{j \neq k} \langle 0 | e_j e_k \exp(i\vec{q} \cdot (\vec{r}_j - \vec{r}_k)) | 0 \rangle, \quad (9)$$

$$Z(Z-1)f_2^p(q) = \sum_{j \neq k} \langle 0 | e_j p_j^x e_k p_k^x \exp(i\vec{q} \cdot (\vec{r}_j - \vec{r}_k)) | 0 \rangle, \quad (10)$$

$$A(A-1)f_2^{\mu}(q) = \sum_{j \neq k} \langle 0 | \mu_j \sigma_j^x \mu_k \sigma_k^x \exp(i\vec{q} \cdot (\vec{r}_j - \vec{r}_k)) | 0 \rangle. \quad (11)$$

The  $p^x$  and  $\sigma^x$  are transverse Cartesian components whose matrix elements are equal to those of  $p^y$  and  $\sigma^y$ . These pair form factors can be evaluated in models of the nuclear ground state or, for low momentum transfer, can be related to photonuclear data through real photon absorption sum rules.

The electron scattering angle used in our measurement ( $20^\circ$ ) was chosen to emphasize the longitudinal response to the nucleus. Thus it is the correlations between proton pairs [Eq. (9)] which plays the decisive role in generating the  $S_{\text{inel}}$  derived from our data. The following subsections discuss the predictions of simple models of the nuclear ground state.

#### A. Harmonic oscillator

The various two-nucleon correlation functions [Eqs. (9)–(11)] that enter the electron scattering sum rule can be evaluated analytically in the oscillator model. The result for carbon is given in Ref. 13.

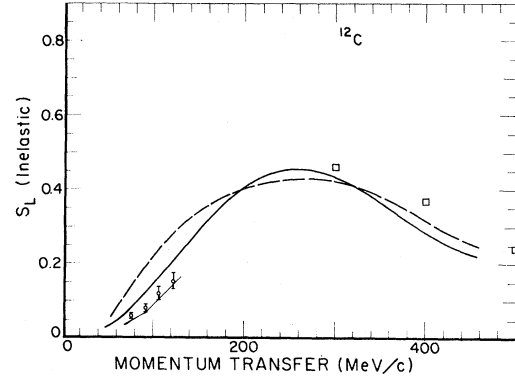


FIG. 4. Longitudinal inelastic sum rule results for  $^{12}\text{C}$  as a function of momentum transfer. The present data (open circles) and Saclay results (open squares) are shown along with  $\gamma_{\text{sum}}$  results which pass through the data, a Fermi gas model calculation (dashed line) with  $k_F = 220$  MeV/c and separation energy = 25 MeV, and harmonic oscillator results (solid line) for  $b = 1.64$  fm.

We have extended these calculations to beryllium and aluminum to compare with the present data. The subtraction of the elastic charge and magnetic form factors with their center-of-mass corrections is an important and delicate step in the computation of  $S_{\text{inel}}$ . This procedure is exact only in the oscillator model.

#### B. Fermi gas

The noninteracting Fermi gas model of nuclear matter is often used to calculate the longitudinal and transverse nuclear response functions in the quasi-free region. However, the infinite gas model becomes increasingly unrealistic at lower momentum transfers because it does not incorporate the collective behavior exhibited by giant multipole resonances, and because the infinite gas does not contain elastic scattering or the correct dependence on momentum transfer characteristic of finite many body systems.<sup>14</sup> Because this model was used in Refs. 1–3 (and forms the basis of the evidence for Coulomb sum rule violation) we include its predictions<sup>15</sup> here for comparison with the higher momentum transfer data in Fig. 4.

The inclusion of meson exchange and isobar creation modifies the predicted gas model response mainly from the interference between one- and two-body contributions. These are small<sup>15,16</sup> effects for  $q < 1$  fm<sup>-1</sup>, especially for the longitudinal response and its energy integral.

#### C. Connection to photon absorption data

In the  $q \rightarrow \omega$  limit the inelastic transverse form factor of electron scattering is related to the real

TABLE I. Inelastic sums ( $S_{\text{inel}}$ ) for each target, along with elastic radiation tail (RT) normalization factors (norm) defined as  $d\sigma_{\text{RT}}(\text{exp})/d\sigma_{\text{RT}}(\text{theory})$  and squared values of excitation energy and vector momentum transfer averaged over the inelastic nuclear continuum (i.e., not including the elastic radiation tail).

$E_i$ (MeV)	200	250	300	350	
${}^9\text{Be}$	$S_{\text{inel}}$	a	0.111	0.125	0.162
	norm		1.12	1.05	1.16
	$q^2$ (MeV $^2/c^2$ )		8107	11108	14874
	$\omega^2$ (MeV $^2$ )		1593	1439	1542
${}^{12}\text{C}$	$S_{\text{inel}}$	0.065	0.090	0.130	0.170
	norm	1.06	1.02	1.07	1.09
	$q^2$	5451	8464	11044	14892
	$\omega^2$	2357	2121	1404	1614
${}^{27}\text{Al}$	$S_{\text{inel}}$	0.099	0.156	0.180	0.211
	norm	0.97	0.95	1.00	1.03
	$q^2$	5519	8365	11090	14838
	$\omega^2$	1407	1931	1428	1478
${}^{51}\text{V}$	$S_{\text{inel}}$	a	0.193	0.219	0.247
	norm		1.00	1.04	1.10
	$q^2$		7843	11152	14704
	$\omega^2$		1236	1475	1220
${}^{90}\text{Zr}$	$S_{\text{inel}}$	a	0.242	0.245	0.294
	norm		0.89	0.95	0.95
	$q^2$		8588	10899	14742
	$\omega^2$		2174	1049	1208
${}^{181}\text{Ta}$	$S_{\text{inel}}$	a	0.397	0.285	0.375
	norm		0.83	1.00	0.97
	$q^2$		8599	10559	14835
	$\omega^2$		2173	517	1370

<sup>a</sup>It was not possible to analyze the data taken with 200 MeV electrons. Primarily the radiation tail could not be treated in a reliable manner.

photon absorption cross section by

$$F_T^2(q, \omega) \Big|_{q \rightarrow \omega} = \frac{\omega \sigma(\omega)}{2\pi^2 \alpha} . \quad (12)$$

This relation holds for electric and magnetic transitions of all multiplicities. At low momentum transfer the nuclear response to electromagnetic radiation is dominated by dipole absorption. The Coulomb dipole form factor is related to the convection current part of the transverse form factor and to the real photon absorption cross section by

$$\begin{aligned} F_C^2(q, \omega) \Big|_{q \rightarrow \omega} &= \frac{1}{2} \frac{q^2}{\omega^2} F_{T,p}^2(q, \omega) \Big|_{q \rightarrow \omega} \\ &= \frac{q^2 \sigma(\omega)}{\omega 4\pi^2 \alpha} . \end{aligned} \quad (13)$$

When energy integrals of the photon cross section are formed,

$$\sigma_n \equiv \int \sigma(\omega) \omega^n d\omega , \quad (14)$$

one has for the inelastic parts of the Coulomb and transverse form factors in the low- $q$  electric dipole limit

$$\mathcal{F}_C^2(q) = \frac{q^2 \sigma_{-1}}{4\pi^2 \alpha} \quad (15)$$

and

$$\mathcal{F}_T^2(q) = \frac{\sigma_{+1}}{2\pi^2 \alpha} . \quad (16)$$

Compilations<sup>17</sup> of photon absorption cross sections and their energy integrals can be used to evaluate Eqs. (15) and (16) to give the  $\gamma_{\text{sum}}$  prediction of the inelastic sum

$$ZS_{\text{inel}}(q) = f_N^2(q_\mu^2) \left\{ \left[ \frac{q_\mu^4}{q^4} \right] \frac{q^2 \sigma_{-1}}{4\pi^2 \alpha} + \left[ \frac{q_\mu^2}{2q^2} + \tan^2 \frac{\theta}{2} \right] \frac{\sigma_{+1}}{2\pi^2 \alpha} \right\}. \quad (17)$$

## VI. COMPARISON OF THEORY AND EXPERIMENT

In Fig. 3 the measured inelastic sums are compared to predictions based on the harmonic oscillator model, the Fermi gas model, and on Eq. (17) called  $\gamma_{\text{sum}}$ . The relative longitudinal and transverse contributions to  $S_{\text{inel}}$  at  $20^\circ$  for  $q \simeq 0.5 \text{ fm}^{-1}$  are, according to predictions, approximately 90% and 10%, respectively. Agreement between experiment and the  $\gamma_{\text{sum}}$  results is good for the lighter nuclei but gets progressively poorer for the heavy nuclei. This behavior may result from the influence of higher multipoles ( $L$ ) in the  $(e, e')$  virtual photon absorption process which grow as  $(qA^{1/3})^{2L-2}$  relative to the dipole absorption mode which was used in deriving the  $\gamma_{\text{sum}}$  results.

The harmonic oscillator (HO) sum rule results are well above experiment for the cases studied ( $^9\text{Be}$ ,  $^{12}\text{C}$ , and  $^{27}\text{Al}$ ). This is not surprising since the simple HO model also gives incorrect predictions for real photon reactions. In particular, the HO model overestimates the electric dipole giant resonance energy and the  $\sigma_{-1}$  sum rule. Random-phase approximation (RPA) calculations which introduce particle-hole ( $ph$ ) pairs in the ground state and mix  $ph$  configurations in the excited states have better agreement with data on photon absorption and muon capture rates.<sup>18</sup> The pair correlations induced by the residual interaction that created the ground state  $ph$  pairs lower the calculated value of  $\sigma_{-1}$  and thus through Eq. (15) decrease the calculated value of  $S_{\text{inel}}$  at low  $q$ .

Fermi gas model (FG) calculations were done for all the elements studied here. For  $^9\text{Be}$  the FG results are significantly above the HO results. This difference decreases for  $^{12}\text{C}$ , and for  $^{27}\text{Al}$  the HO and FG results essentially agree. One might expect this behavior in going to heavy nuclei since the FG model best describes infinite nuclear matter. The failure of the FG model to describe the  $^{181}\text{Ta}$  results shown in Fig. 3 is therefore surprising, but may, in fact, stem from inadequacies in the radiation tail theory, the most serious concern in the present experiment.

In Fig. 4 and HO and FG predictions for  $^{12}\text{C}$  are given for just the longitudinal part of  $S_{\text{inel}}$  over a

large span of momentum transfer. High momentum transfer points<sup>3</sup> for which a longitudinal-transverse separation was made are shown together with our four low momentum points reduced by between 5% and 10% to eliminate transverse contributions. We find it interesting that the FG and HO calculations agree reasonably well. One should recall that explicit sum rule calculations sometimes neglect terms of order  $(q/M)^4$  which come from the electron spin-orbit interactions. In particular, this was done for the present HO calculations. Even in this approximation we find that the relativistic effects  $\mathcal{O}(q^2/M^2)$  are responsible for reducing  $S_{\text{inel}}$  from 1.0 at high  $q$  to less than 0.5. One can therefore speculate that neglecting terms of order  $q^4/M^4$  with respect to terms of order  $q^2/M^2$  can lead to errors of order  $q^2/M^2 \times 0.5$ . At  $q=400 \text{ MeV}/c$  these errors are of order 0.1. For the FG calculations to obtain the sum rule result, we performed an excitation energy integral over the quasielastic  $(e, e')$  calculation of Van Orden<sup>15</sup> which includes the higher order  $(q^4/M^4)$  terms. The differences between the HO and FG calculations at high  $q$  may be due to this latter effect or possibly due to an inadequate treatment of long range correlations between nucleons. In any event this difference is probably a reasonable measure of uncertainty in the theory at high  $q$ .

Our original motivation for the present sum rule study was based on measurement of quasifree electron scattering from medium- $A$  nuclei ( $A=40-54$ ) which indicated that the measured  $S_L(q)$  at  $q \simeq 400 \text{ MeV}/c$  was only half of the sum-rule result.<sup>1,2</sup> Recent measurements<sup>8</sup> indicate that this discrepancy may be significantly less than earlier thought, and may in fact be within theoretical uncertainties of the FG calculations. Our present low- $q$  data for  $^{51}\text{V}$  are in good agreement with the FG predictions.

A comment regarding the radiation tail calculation is called for since it is overwhelmingly important to the present effort and certainly significant even to higher- $q$  experiments. Our radiation tail calculations are exact only in first Born approximation. Attempts to include Coulomb distortion effects have been made by using measured form factors or phase shift calculations where theory calls for the Born approximation form factors. In fact, this is only a guess as to how to deal with distortion effects in the radiation process for a finite nucleus. There are, for example, second-order Born terms and effects due to Coulomb distortion of the electron wave that are neglected in the radiation process. Another effect which enters the radiation tail calculation rather strongly in the present experiment is the requirement that the electron-nucleus form factor needs to be specified over roughly twice momentum transfer corresponding to nonradiative electron scattering.

The reason for this effect is that electrons can, for example, scatter at twice the nominal scattering angle of  $20^\circ$ , and, by emission of a hard photon, recoil in such a way as to finally emerge at a  $20^\circ$  scattering angle. This effect would not be dealt with in any inelastic radiative unfolding procedure because, generally, the peaking approximation to radiative scattering in which radiation is only emitted along the direction of electron travel is used.

One final comment regarding Coulomb distortion effects on the very inelastic process under study is also called for. We have examined this effect on the sum rule by using a distorted wave (DW) calculation of the  $(e, e')$  process, assigning a strength and excitation energy to each multipole given by a hydrodynamical model (for the electric multipoles only), and compared this result with a similar calculation using plane wave Born approximation (PW). Deviations from unity in the ratio of DW to PW results range from less than 1% for  $^9\text{Be}$  at 350 MeV electron energy, to more than 20% for  $^{181}\text{Ta}$  at the same energy. In order to compare the present measurements with BA theory we have chosen to plot the data at momentum transfer values given by

$$q_{\text{eff}} = q \left[ 1 + \frac{3}{2} \left( \frac{3}{5} \right)^{1/2} \frac{Z\alpha}{E_i \langle r^2 \rangle^{1/2}} \right].$$

To appreciate the magnitude of Coulomb distortion effects we have shown in Fig. 3 the raw data for  $^{51}\text{V}$ ,  $^{90}\text{Zr}$ , and  $^{181}\text{Ta}$  as well as the same data multiplied by the above-mentioned distortion factor PW/DW.

The purpose of this experiment was to compare theoretical sum rules and experiment at low momentum transfers as a complement to the high- $q$  data which revealed an apparent discrepancy between<sup>1,2</sup> experiment and theory. We are forced to conclude that the calculations which we considered do not give uniform agreement with the present data. We have examined several possible sources of difficulties which may be valuable for future studies. Included among these is the discovery of a source of previously unaccounted instrumental background<sup>8</sup> which has an effect on earlier results.<sup>1,2</sup> The sum rule of Eq. (5) is not a strict conservation rule, but a model is required for its interpretation. Considering the ability of experiments to measure  $S_{\text{inel}}$  with all the data analyses involved and the assumptions inherent in the theory, we feel that it is still premature to say that serious sum rule violations exist outside conventional nuclear structure effects.

<sup>1</sup>R. Altemus, A. Cafolla, D. Day, J. S. McCarthy, R. R. Whitney, and J. E. Wise, *Phys. Rev. Lett.* **44**, 965 (1980).

<sup>2</sup>M. Deady, Ph.d. thesis, Massachusetts Institute of Technology, 1981.

<sup>3</sup>P. Barreau, M. Bernheim, M. Brussel, G. P. Capitani, J. Duclos, J. M. Finn, S. Frullani, F. Garibaldi, D. Isabelle, E. Jans, J. Morgenstern, J. Mougey, D. Royer, B. Saghai, E. de Sanctis, I. Sick, D. Tarnowski, S. Turck-Chieze, and P. D. Zimmerman, *Nucl. Phys.* **A358**, 287c (1981).

<sup>4</sup>W. Bertozzi, M. V. Hynes, C. P. Sargent, W. Turchinetz, and C. Williamson, *Nucl. Instrum. Methods* **162**, 211 (1979).

<sup>5</sup>S. Henning and L. Svensson, University of Lund Report LUND 6, 1979.

<sup>6</sup>L. W. Mo and Y. S. Tsai, *Rev. Mod. Phys.* **41**, 205 (1969); and SLAC-PUB-848, 1971.

<sup>7</sup>E. Lomon, in Massachusetts Institute of Technology Report TID-24667, edited by W. Bertozzi and S. Kowlaski, 1967, p. 221.

<sup>8</sup>J.-O. Adler, K. Hansen, and B. Schroder (unpublished); R. Roy Whitney and Rosemary Altemus, private communication.

<sup>9</sup>S. D. Drell and C. L. Schwartz, *Phys. Rev.* **112**, 568 (1958).

<sup>10</sup>K. W. McVoy and L. VanHove, *Phys. Rev.* **125**, 1034 (1962).

<sup>11</sup>W. Czyz, L. Lesniak, and A. Malecki, *Ann. Phys. (N.Y.)* **42**, 97 (1967); **42**, 119 (1967).

<sup>12</sup>J. S. O'Connell, *Phys. Lett.* **32B**, 323 (1970).

<sup>13</sup>J. W. Lightbody, Jr., *Phys. Lett.* **33B**, 129 (1970).

<sup>14</sup>L. L. Foldy and J. D. Walecka, *Nuovo Cimento* **36**, 1257 (1965).

<sup>15</sup>J. W. Van Orden and T. W. Donnelly, *Ann. Phys. (N.Y.)* **131**, 451 (1981).

<sup>16</sup>M. Kohno and N. Ohtsuka, *Phys. Lett.* **98B**, 335 (1981).

<sup>17</sup>E. G. Fuller, private communication.

<sup>18</sup>Nguyen Van Giai, N. Auerbach, and A. Z. Mekjian, *Phys. Rev. Lett.* **46**, 1444 (1981).